Patches of Mutant p53-Immunoreactive Epidermal Cells Induced by Chronic UVB Irradiation Harbor the Same p53 Mutations as Squamous Cell Carcinomas in the Skin of Hairless SKH-1 Mice

Pavel Kramata, Yao-Ping Lu, You-Rong Lou, Rayvita N. Singh, Sherry M. Kwon, and Allan H. Conney

Susan Lehman Cullman Laboratory for Cancer Research, Department of Chemical Biology, Ernest Mario School of Pharmacy, Rutgers, The State University of New Jersey, Piscataway, New Jersey

Abstract

Treatment of SKH-1 hairless mice with UVB (30 mJ/cm^2) twice a week for 20 weeks results in the formation of cellular patches, long before the appearance of tumors, that are visualized in epidermal sheets with an antibody (PAb240) recognizing mutated p53 protein. Direct sequencing analysis of the whole coding region of the *p53* gene (exons 2-11) detected one or two mutations in 64.4% of 104 analyzed patches and no mutations in nonstained adjacent normal controls. Homozygous mutation was detected in 22.4% of the mutant patches. Except for two nonsense mutations, all others were missense (exons 4-9) and mostly (95.5%) at the DNA-binding domain. Primer extension analysis of cloned PCR fragments found three of four double-mutated patches harboring different mutations in separate alleles. All mutation hotspots reported earlier in UVB-induced mouse squamous cell carcinomas (SCC) at codons 270 (Arg → Cys), 149 (Pro → Ser), 275 (Pro → Leu and Pro → Ser), and 176 (His → Tyr) with a frequency of 32.1%, 7.1%, 14.7%, and 3.2% were detected in epidermal patches at a frequency 47.7%, 9.1%, 4.5%, and 2.3%, respectively. Mutations at codons 210 and 191 found in patches at respective frequencies of 8.0% and 4.5% were not previously detected in UVB-induced mouse SCC. In summary, (a) the p53 mutation profile of UVB-induced skin patches and SCC was very similar suggesting that patches are precursor lesions for SCC, (b) a small number of patches harbored mutations that were not before observed in SCC from UVB-treated mice, and (c) about 36% of the patches did not harbor a p53 mutation. (Cancer Res 2005; 65(9): 3577-85)

Introduction

The causal role of solar radiation in the formation of nonmelanoma skin cancers (basal and squamous cell carcinomas, SCC) in humans is well known (1). Experiments with a hairless mouse model of skin carcinogenesis showed the dependence of skin tumor development on the dose and duration of UV radiation (2) and identified UVB (280-320 nm) as the most mutagenic and carcinogenic region of the solar spectrum (3). The link between mutagenic effects of UVB light and skin cancer has been shown mainly by the analyses of mutation spectra of the *p53* gene in mouse (4) and human skin cancers (5) harboring mostly C → T transition mutations and CC → TT tandem mutations located at dipyrimidine sites that are typical for UVB mutagenesis (6).

The *p53* gene is the most commonly mutated gene in human cancers (7, 8). It encodes for a multifunctional transcription factor participating in the activation of genes that induce cell cycle arrest, DNA repair, and apoptosis following DNA damage. In nonmelanoma skin cancers, the incidence of p53 mutations ranges from 50% to over 90% both in human (9) and mouse lesions (10–13). Such a high frequency argues for a critical role of p53 in skin carcinogenesis. Not surprisingly, p53 knockout mice show much higher susceptibility to skin cancer induction by UV light than their wild-type counterparts (14).

UV-induced skin carcinogenesis is a complex sequential process that likely involves mutagenic changes in several genes including proto-oncogenes and tumor suppressors. Expansion of a cellular clone that gains a selective growth advantage and increased resistance to UV-induced apoptosis by an initial mutagenic event in a critical gene(s) is considered a starting point of skin tumor development (6). Patches of morphologically normal keratinocytes that stain positively with an antibody recognizing an altered conformation of the mutant form of p53 protein may represent such an early step. These patches are common in normal human skin, and they are larger and more numerous in sun-exposed skin than in sun-shielded skin (15). Similarly, numerous p53-positive patches are present in chronically UVB-irradiated mouse skin (16); their growth is directly proportional to the UVB dose (17) and their expansion to adjacent keratinocyte compartments requires continuous UVB treatment (18). The question of whether these patches constitute early precursors of malignant skin tumors has been extensively debated. Their density is significantly higher in the proximity of SCCs compared with basal cell carcinomas or benign melanocytic naevi (19), and there is a correlation between the frequency of patches and the risk of SCCs in mice (17). Finding identical p53 mutations in patches and tumors would strongly support the concept that mutant p53–positive patches are early precursors of tumors. Although some studies have found different p53 mutations in patches and skin tumors present simultaneously in the same human samples (20, 21) suggesting no genetic link between these lesions, several skin tumor p53 mutation hotspots have been detected in human (15) and mouse (16, 18) skin patches as well as in a recent and extensive study of patches of human p53–immunostained epidermal keratinocytes (22). It seems certain

Note: A.H. Conney is the William M. and Myrle W. Garbe Professor of Cancer and Leukemia Research.

Requests for reprints: Pavel Kramata, Susan Lehman Cullman Laboratory for Cancer Research, Department of Chemical Biology, Ernest Mario School of Pharmacy, Rutgers, The State University of New Jersey, 164 Frelinghuysen Road, Piscataway, NJ 08854-8020. Phone: 732-445-3400, ext. 238; Fax: 732-445-0687; E-mail: kramata@rci.rutgers.edu.

that not all patches of keratinocytes expressing the mutant form of p53 develop into carcinomas because their high numbers in chronically UV-irradiated skin (20-50 per cm^2 in humans; ref. 15) do not translate into similar numbers of eventually developed tumors. It is possible that only certain p53 mutations predispose mutant keratinocytes to malignant transformation. To test this hypothesis, we have analyzed p53 mutations in the whole *p53* gene (exons 2-11) in 104 samples of epidermal patches of cells positively stained with an antibody recognizing the mutant form of p53 protein (PAb240) from chronically UVB-irradiated hairless SKH-1 mice long before tumor formation, and we have compared the mutation spectrum data obtained from these patches to the extensive data published from p53 mutation analysis of skin SCCs induced in the same mouse model by chronic UVB light exposure (10) or with a solar simulator (12, 13).

Materials and Methods

Animals and UV treatment. Female SKH-1 hairless mice (6-7 weeks old, Charles River Breeding Laboratories, Kingston, NY) were exposed to 30 mJ/cm^2 of UVB light twice a week (Tuesday and Friday) for 20 weeks. UV lamps (FS72T12-UVB-HO; National Biological Co., Twinsburg, OH) emitted UVB (280-320 nm; 75-80% of total energy) and UVA (320-375 nm; 20-25% of total energy). The dose was quantified with a UVB Spectra 305 dosimeter (Daevlin Co., Byran, OH). The radiation was further calibrated with a model IL-1700 research radiometer/photometer (International Light, Inc., Neburgport, MA). The mice were given Purina Laboratory Chow 5001 diet (Ralston-Purina Co., St. Louis, MO) *ad libitum*, were kept on a 12-hour light/12-hour dark cycle, and sacrificed by cervical dislocation.

Immunohistochemistry. Dorsal skin samples (2 × 4 cm) removed from animal trunks were treated with thermolysin and $CaCl_2$ overnight and fixed in cold acetone. The epidermis was attached to a Hybond membrane and separated from the dermis with a pair of tweezers. Endogenous peroxidase was blocked with H_2O_2 in methanol. Nonspecific binding of antibody was blocked with normal rabbit serum, bovine serum albumin, and saponin. The epidermal sheet was incubated either with monoclonal p53 antibody PAb240 (NCL-p53-240) that recognizes mutant p53 protein (Novocastra, Newcastle upon Tyne, United Kingdom) or PAb1620 (OP33) that recognizes wild-type p53 protein (Oncogene Research Products, Uniondale, NY). Following application of biotinylated secondary antibodies and avidin-biotin-peroxidase complex, the sheets were stained with 3,3′-diaminobenzidine.

Microdissection, DNA amplification, and sequencing. Samples of ~100 to 1,000 cells were isolated from clones of skin cells in stained epidermal sheets under the microdissecting microscope using a 30-gauge needle (Becton Dickinson, Rutherford, NJ) and a micromanipulator (Narishige MO-203, Tokyo, Japan). Samples were placed into 20 μL of 10 mmol/L Tris-HCl (pH 8.5) and 1% Tween 80 and incubated for 16 hours at 65°C with 3.2 μg/μL proteinase K (PCR grade, Roche Biochemicals, Indianapolis, IN). Proteinase K was inactivated for 15 minutes at 95°C and sample aliquots were directly used for DNA amplification (one tenth of the reaction volume). Fragments 331, 548, 507, 322, 495, 300, and 249 bp (encompassing exons 2, 3 + 4, 5 + 6, 7, 8 + 9, 10, and 11, respectively) were individually amplified in PCR reaction mixtures (25 μL) containing 0.025 units/μL HotStarTaq DNA polymerase (Qiagen, Valencia, CA), Qiagen reaction buffer (1×) with 1.5 mmol/L $MgCl_2$, 200 μmol/L of each deoxynucleotide triphosphate (dNTP), and 0.2 μmol/L of each primer. Cycling conditions were as follows: after the initial 15 minutes at 94°C, there were 40 cycles (94°C, 30 seconds/55°C, 30 seconds/72°C, 45 seconds) and a final 7-minute step at 72°C. Primers (IDT, Coralville, IA) located in introns had the following sequences: Ex2for, 5′-ATTTCCCTACTGGATGTCCCACC; Ex2rev, 5′-TTACAGACACCCAACACCATACC; Ex3,4for, 5′-CCTGGGATAAGTGAGATTCTGTC; Ex3,4rev, 5′-GGCACAGTCTACAGGCTGAAGAG; Ex5,6for, 5′-CCTTGACACCTGATCGTTACTCG; Ex5,6rev, 5′-AGAAAGTCAACATCAGTCTAGGC; Ex7for, 5′-TGTGCCGAACAGGTGGAATATCC; Ex7rev, 5′-ACTCGTGGAACAGAAACAGGCAG; Ex8,9for, 5′-GGCCTAGTTTACACACAGTCAGG; Ex8,9rev, 5′-CACGGCTAGAGATAAAGCCACTG; Ex10for, 5′-GCCAGCTTAAGTTGGGAACCAAC; Ex10rev, 5′-ATCTTTCACTACAAAGGCTGAGC; Ex11for, 5′-CTAGAGCCTTCCAAGCCTTGATC; Ex11rev, 5′-AGGATTGTGTCTCAGCCCTGAAG.

Amplified fragments were visualized on a 1.5% agarose gel stained with ethidium bromide. Before sequencing, primers and dNTPs in PCR reaction mixtures were digested with exonuclease I and shrimp alkaline phosphatase (ExoSAP-IT, U.S. Biochemical Co., Cleveland, OH) at 37°C for 15 minutes, and the enzymes were deactivated at 80°C for 15 minutes. DNA sequencing was done using the same primers and BigDye sequencing kit from Applied Biosystems (Foster City, CA) and analyzed with automatic sequencer ABI Prism 3100 Genetic Analyzer (DNA Sequencing Core Facility, University of Medicine and Dentistry of New Jersey, Piscataway, NJ). Sequencing waveforms were processed using Chromas 2.22 computer program (Technelysium, Tewantin, Australia). A mutation appeared as a vertical double signal (peak) at the same nucleotide position. Two sequences of each sample (generated with forward and reverse primers) were compared with a standard normal mouse p53 sequence retrieved from the Genbank (accession no. AC074149, *Mus musculus* clone RP23-114M1) by the sequence alignment program MultiAlign available online at http://prodes.toulouse.inra.fr/multalin/multalin.html that uses a published algorithm (23). Mutation changes that appeared on both parallel sequences were scored. The position was considered mutated when the mutant signal represented at least 25% of the total sequencing signal at the position with a negligible level of noise in the background. A complete loss of the wild-type sequence should theoretically yield a 100% mutant signal at the mutation site. To compensate for the possibility of contamination by normal cellular DNA, a mutation was scored as homozygous when a mutant signal was >75% of the total signal at the mutation site.

Cloning of PCR products and determination of mutations by primer extension minisequencing analysis. PCR fragments from selected samples harboring two p53 mutations were cloned into the pCR2.1-TOPO vector by TOPO TA Cloning according to the manufacturer's instructions (Invitrogen, Carlsbad, CA). Following transfection into competent *Escherichia coli* (TOP 10, Invitrogen), 25 to 30 individual white colonies (white-blue selection) were picked, grown in 2-mL cultures and the plasmids isolated by the QIAprep Spin Miniprep Kit (Qiagen). The presence of a mutant base or the wild-type base at the mutant sites was analyzed by primer extension minisequencing analysis as described before (24). Briefly, the 3′ terminus of a ^{32}P-labeled primer (50 nmol/L), annealed to the plasmid template (200 nmol/L) one nucleotide before the mutated spot, was extended with Thermo-Sequenase DNA polymerase (0.4 units/μL, U.S. Biochemical) in a thermocycling reaction (95°C, 30 seconds; 50°C, 10 seconds; 72°C, 10 seconds; 25 cycles and initial 1 minute at 95°C). The reaction (10 μL) contained a single dNTP (10 μmol/L) complementary to the examined base and dideoxynucleotide triphosphate (ddNTP, 1 μmol/L) in dependence on the particular sequence. The primer could be extended with dNTP only when the examined base was present and terminated by ddNTP incorporation or terminated with ddNTP immediately in the first step. After adding a formamide buffer (95% formamide, 20 mmol/L EDTA, 0.05% bromophenol blue), the reaction products were separated on 15% PAGE in Tris-borate EDTA buffer and visualized by autoradiography. The sequence of the primers, dNTP and ddNTP, used for the detection of mutations at sites 174, 238, 245, 270, and 306 is shown in Table 1.

Results

p53 mutation profile of individual p53-immunopositive skin patches. Hairless SKH-1 mice chronically irradiated with a low dose of UVB light (30 mJ/cm^2, twice a week for 20 weeks) develop patches of keratinocytes in the dorsal area of skin that react positively with an antibody against the mutated form of p53 (PAb240) but not with an antibody against wild-type p53 (PAb1620; Fig. 1). These patches start appearing as clusters of four to eight cells in the skin after 4 weeks of UVB treatment. Samples for our

Table 1. Primers, dNTP and ddNTP, used in the primer extension assay to determine p53 mutations at cloned PCR fragments

Name	Primer sequence (5′ → 3′)	Mutation site*	dNTP/ddNTP in assay	
			Wild type	Mutant
174for	GGAGGTCGTGAGACGCTGCC	C/TCCA	dC/ddA, ddT	dT/ddC
238for	ACAAGTACATGTGTAATAGCT	C/TCT	dC/ddT	dT/ddC
245rev	TGGTAAGGATAGGTCGGC	G/CGT	dG/ddT, ddC	dC/ddG
270for	CGGGACAGCTTTGAGGTT	C/TGT	dC/ddG, ddT	dT/ddG, ddC
306for	TCTCCTTCCACAGCGCTG	C/TCCA	dC/ddA, ddT	dT/ddC

*Sequence following the 3′ terminus of the primer.

study were taken from eight mice treated with UVB for 20 weeks. Although these animals have no tumors, they have a high risk of developing SCC over the next several months in the absence of further UVB treatment. Each of 104 patches analyzed (13 ± 2 per mouse), containing ~100 to 1,000 cells per patch, was isolated with a thin needle and a micromanipulator under a microdissecting microscope and each patch was treated as described in Materials and Methods. Two to three samples of normal, nonstained skin were also taken from each mouse as a control. Mutations in the whole *p53* gene (exons 2-11) were detected by direct sequencing of individually PCR-amplified DNA fragments as described in Materials and Methods. The analysis was done without single-strand conformational polymorphism (SSCP) prescreening because (a) compact cell patches visualized with a PAb240 antibody staining provide DNA samples with potentially highly enriched mutant p53 sequences and (b) SSCP analysis may underestimate the number of p53 mutations (11) as its efficiency depends on the size of DNA fragments, the analyzed sequence, and the electrophoresis running conditions (25, 26).

One or two p53 mutations were found in 64.4% of 104 analyzed patches and no mutations were found in nonstained normal controls (Table 2). With the exception of two nonsense mutations, all detected alterations changed the amino acid (missense mutations). They were located between exons 4 and 9 and mostly concentrated into several hotspots (codons 149, 191, 210, 270, and 275). All of the hotspots and the majority of other mutations (95.5% overall) were at the p53 central core DNA-binding domain (amino acids 102-304; ref. 27). No mutations were found in exons 2, 3, 10, or 11.

The most prevalent mutation hotspot changing Arg to Cys at position 270 (Fig. 2*A*) was detected in 42 samples representing 62.7% of mutated patches (Table 2). Thirty-one samples in this group harbored this hotspot as the only mutation; nine of them exhibited the intensity of the mutant signal >75% of the total signal at the mutant position (homozygous mutation; Fig. 2*B*) indicating a loss of the normal *p53* allele in the patch. This number may be an underestimate considering the possibility of contamination by normal cells. The remaining 11 samples contained the hotspot 270 and another mutation. Interestingly, two of them were also homozygous for the mutant 270, which implies the formation of two mutations in the same *p53* allele.

The minor mutation hotspots at codons 149 (Pro → Ser; Fig. 2*C*), 210 (Arg → Cys; Fig. 2*D*), 275 (Pro → Ser and Pro → Leu), and 191 (Leu → Ser and Leu → His) were all found in combination with another mutation, but only those at codons 149, 210, and 275 (Pro → Ser) were detected as single mutations (Table 2). We assume that the mutations found in single-mutated patches are critical for the patch selection and could thus be considered as "driving" mutations in double-mutated patches. The functional contribution of a second mutation is difficult to assess. Two driving mutations combined in one patch, when located on separate alleles, would likely result in

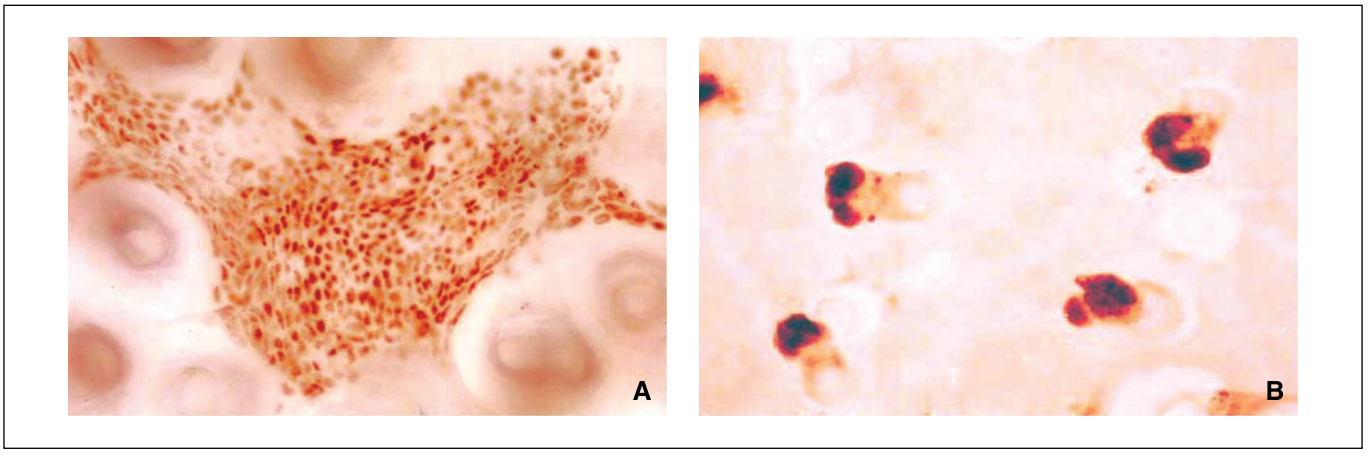

Figure 1. Mouse epidermal sheets stained with antibodies (*A*) PAb240 recognizing mutant p53 and (*B*) PAb1620 recognizing wild-type p53. Hairless mice SKH-1 were treated with an UVB light dose of 30 mJ/cm^2 twice a week for 20 weeks, and the epidermal sheets were stained 72 hours after the last irradiation. The large dark areas are hair follicles that are nonspecifically stained.

eliminating the normal p53 function. The less frequent or rare mutations, especially when located on the same allele, may be mere "hitchhikers" that were coselected without functional consequences. The distribution of two mutations between alleles from several samples is examined in the following section.

The results show that p53 mutations in patches of epidermal cells with mutant p53 protein induced by chronic UVB irradiation in mouse skin are almost exclusively missense, concentrated into several hotspots positioned in the DNA-binding domain and homozygous in more than one fifth of the samples. The results also show a remarkable diversity of the samples, with almost every other analyzed patch having a different p53 mutational profile, and show that single-mutated patches with a heterozygous mutation at position 270 are overwhelmingly dominant.

Table 2. p53 mutations in individual UVB-induced epidermal cell patches of hairless mice

	No. samples/ samples with a homozygous mutation*
One mutation	
275 $Cct^{Pro} \rightarrow Tct^{Ser}$	1
274 $tGc^{Cys} \rightarrow tTc^{Phe}$	1/1
270 $Cgt^{Arg} \rightarrow Tgt^{Cys}$	31/9
262 $cTg^{Leu} \rightarrow cCg^{Pro}$	1
245 $Cgc^{Arg} \rightarrow Agc^{Ser}$	1/1
245 $Cgc^{Arg} \rightarrow Tgc^{Cys}$	1
238 $TCc^{Ser} \rightarrow CTc^{Leu}$	1
235 $Tgt^{Cys} \rightarrow Agt^{Ser}$	1
210 $Cgc^{Arg} \rightarrow Tgc^{Cys}$	3
176 $Cat^{His} \rightarrow Tat^{Tyr}$	1
149 $Cca^{Pro} \rightarrow Tca^{Ser}$	4/2
101 $Cag^{Gln} \rightarrow Tag^{Term}$	1
Two mutations	
275 $cCt^{Pro} \rightarrow cTt^{Leu}$ + 210 $Cgc^{Arg} \rightarrow Tgc^{Cys}$	1
275 $cCt^{Pro} \rightarrow cTt^{Leu}$ + 174 $cCc^{Pro} \rightarrow cTc^{Leu}$	1
275 $Cct^{Pro} \rightarrow Tct^{Ser}$ + 127 $Ctc^{Leu} \rightarrow Ttc^{Phe}$	1
270 $Cgt^{Arg} \rightarrow Tgt^{Cys}$ + 306 $Ccc^{Pro} \rightarrow Tcc^{Ser}$	1 /1 at 270
270 $Cgt^{Arg} \rightarrow Tgt^{Cys}$ + 245 $Cgc^{Arg} \rightarrow Ggc^{Gly}$	1
270 $Cgt^{Arg} \rightarrow Tgt^{Cys}$ + 238 $tCc^{Ser} \rightarrow tTc^{Phe}$	1
270 $Cgt^{Arg} \rightarrow Tgt^{Cys}$ + 191 $CTt^{Leu} \rightarrow TCt^{Ser}$	2
270 $Cgt^{Arg} \rightarrow Tgt^{Cys}$ + 174 $Ccc^{Pro} \rightarrow Tcc^{Ser}$	1
270 $Cgt^{Arg} \rightarrow Tgt^{Cys}$ + 149 $Cca^{Pro} \rightarrow Tca^{Ser}$	4 /1 at 270
270 $Cgt^{Arg} \rightarrow Tgt^{Cys}$ + 110 $ttC^{Phe} \rightarrow ttA^{Leu}$	1
261 $Ctt^{Leu} \rightarrow Ttt^{Phe}$ + 210 $Cgc^{Arg} \rightarrow Tgc^{Cys}$	1
210 $Cgc^{Arg} \rightarrow Tgc^{Cys}$ + 110 $Ttc^{Phe} \rightarrow Atc^{Ile}$	1
210 $Cgc^{Arg} \rightarrow Tgc^{Cys}$ + 95 $Cct^{Pro} \rightarrow Tct^{Ser}$	1
191 $cTt^{Leu} \rightarrow cAt^{His}$ + 176 $Cat^{His} \rightarrow Tat^{Tyr}$	1
191 $cTt^{Leu} \rightarrow cAt^{His}$ + 127 $Ctc^{Leu} \rightarrow Ttc^{Phe}$	1
60 $gCc^{Ala} \rightarrow gGc^{Gly}$ + 62 $Cga^{Arg} \rightarrow Tga^{Term}$	1
Mutant samples	67
With a different p53 profile	32
With at least one SCC hotspot mutation (%)	77.6
With more than one mutation (%)	29.9
With a mutation at 270 (%)	62.7
With a homozygous mutation (%)	22.4
With a homozygous mutation at 270 (%)	16.4

*Samples with the mutant signal >75% of the total signal at the mutant site.

Distribution of p53 mutations between alleles in double-mutant cellular skin patches. To determine the distribution of two p53 mutations between alleles in four double-mutated patches, we cloned PCR fragments harboring both mutations and did a primer extension minisequencing analysis of the mutant sites in 26 to 30 individual clones from each sample as described in Materials and Methods and Fig. 3. We analyzed mutants harboring mutation at codon 270 (Arg → Cys) in combination with mutations at codons 174 (Pro → Ser), 238 (Ser → Phe), 245 (Arg → Gly), or 306 (Pro → Ser).

Results of the analysis are shown in Table 3. In samples 270-174 and 270-238, the mutations were always found in different alleles indicating that the patches were likely composed of a homogenous population of cells bearing one mutation on each *p53* allele and losing thus the normal p53 function. In sample 270-245, the mutations were found in different alleles with the exception of one clone where both mutations were located in the same allele (Fig. 3). This result was confirmed by direct sequencing of the clone (data not shown). To account for a significant difference in the number of clones with a single-mutated allele (15 times with mutation 270 and six times with mutation 245), a relatively high level of an allele with no mutation (eight times) and the presence of a double-mutated allele in this sample, we concluded that the analyzed patch might contain a mixture of three kinds of cells possibly reflecting sequential development of the patch: a heterozygous 270 mutant, a heterozygous 270-245 mutant with both mutations positioned in one allele, and a double 270-245 mutant with each mutation in a different allele. Although it is not clear how a mutation could be transferred between alleles, a process such as homologous recombination seems most likely. In sample 270-306, the alleles were mostly double mutated, but there was also a portion of single 270 mutants. We interpret this finding as a patch composed of cells bearing one double-mutant allele and one single-mutant allele. Contamination of the samples with normal cells may be responsible for the detection of alleles with no mutation.

The data support the hypothesis that most of the double-mutated patches bear mutations at two different alleles and that their selection is driven by a loss of normal p53 function. On the other hand, probably a small portion of double mutants harbors two mutations on one allele, as shown for 270-306 sample, with the second mutation having a questionable functional effect. Whether some of these "second" mutations could be transferred onto the normal allele resulting in the loss of the wild-type p53, as inferred from the analysis of sample 270-245, is a matter of speculation.

Comparison of mutation profiles of the *p53* gene from epidermal cell patches and mouse squamous cell carcinomas. The positions, amino acid changes, frequency of mutations, and types of base substitutions were compared with results of an extensive p53 sequencing study of SCC induced by UVB-light in the same mouse model (10). Results of two smaller studies that used a solar simulator to induce tumors (12, 13) were also included.

The comparison shows a remarkable similarity in the mutation profile between patches and tumors (Table 4). All mutation hotspots (frequency >3% of the total number of mutations) detected in SCC at codons 270 (Arg → Cys), 275 (Pro → Leu and Pro → Ser), 149 (Pro → Ser), and 176 (His → Tyr) were also present in epidermal skin patches. At least one SCC mutation hotspot was detected in 77.6% of the mutant patches (Table 2). The relative frequency of mutations at codons 270, 275, 149, and 176 in patches was 47.7%, 4.5%, 9.1%, and 2.3%, respectively, compared with 32.1%, 14.7%, 7.1%, and 3.2%, respectively, reported in SCC. Two mutated

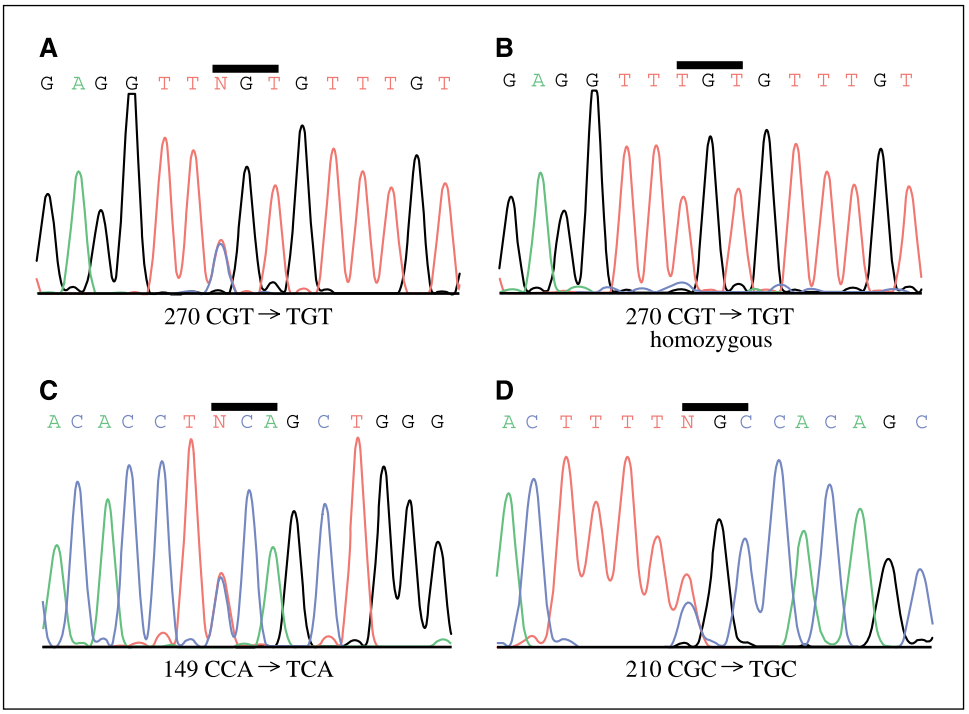

Figure 2. Mutation hotspots in the *p53* gene of mouse epidermal skin patches induced by chronic UVB irradiation that stained positively with an antibody to mutant p53: (*A*) 270 (Arg → Cys); (*B*) homozygous 270 (Arg → Cys); (*C*) 149 (Pro → Ser); (*D*) 210 (Arg → Cys). Individual DNA fragments encompassing exons 2 to 11 of the mouse p53 were amplified and directly sequenced as described in Materials and Methods. Mutations were identified by visual inspection of the sequencing waveforms followed by a computer sequence alignment.

codons, 210 (Arg → Cys) and 191 (Leu → His and Leu → Ser), found in patches with the respective relative frequency of 8.0% and 4.5%, were not detected in the major p53-sequencing study of SCC (10). Interestingly, a mutation at codon 210 (Arg → Cys) was detected in SCC induced by a solar simulator (12).

It is possible that skin tumor cells, being exposed to the mutagenic effects of UV light for much longer time than skin patches and also potentially subject to increasing internal mutability, would acquire additional, possibly functionally silent, p53 mutations during tumor development. The relative frequency of major mutation hotspots in early skin patches should then be higher than in tumor cells. The relative frequency of the mutation hotspot 270 found in skin patches (47.7%) was significantly higher than in skin tumors (32.1%; $P < 0.02$, Fisher's exact test), but the numbers were comparable for the mutation hotspots 149 and 176 (9.1% and 2.3% in skin patches versus 7.1% and 3.2% in tumors). Surprisingly, the relative frequency of mutations at position 275 was significantly lower in the skin patches (4.5%) than in tumors (14.7%; $P < 0.02$, Fisher's exact test). If we assume that antibody PAb240 to the mutant form of p53 used in our study and antibody CM-5 used in the tumor study react to the 275 mutant with a similar affinity, the difference between skin patches and tumors may indicate a higher "tumorigenic" potential of cells harboring p53 mutation at codon 275 leading to their enrichment in tumors.

The distribution of UVB-induced base substitutions in p53 mutations of patches and SCC (10) is compared in Table 5. Similar to tumors, most of the detected mutations in patches were C → T transitions located at dipyrimidine sites on the nontranscribed strand of the gene confirming the mutagenic role of UV light in the induction of these mutations. Interestingly, tandem double substitutions, a hallmark of UV light mutagenesis (28), accounted only for 4.5% of mutations in patches compared with 10.3% in

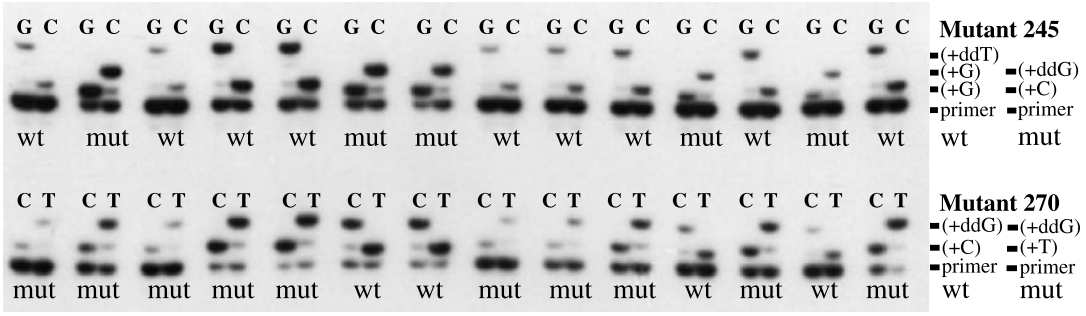

Figure 3. Minisequencing analysis of cloned PCR fragments from skin patches harboring mutations at codons 270 and 245. PCR fragments encompassing both mutation sites were cloned in a plasmid and transformed into bacteria. Bacterial colonies were randomly picked, and following plasmid isolation the sequence at the sites of mutations was analyzed by primer extension assay as described in Materials and Methods. The sample is either mutant or wild type based on the extension of the primer with a mixture of dNTP and ddNTP as shown in Table 1. The 3′ end of the annealed primer is positioned one nucleotide before the analyzed site.

Table 3. Distribution of mutations between the *p53* alleles of four double-mutated epidermal cell patches (position 270 and M, a second mutation)

Mutations in alleles	Amino acid position of a second p53 mutation (M)			
	174	238	245	306
270 only	10	10	15	10
M only	11	16	6	0
270 and M	0	0	1	14
No mutation (wild type)	6	0	8	3
No. analyzed clones	27	26	30	27

NOTE: PCR-amplified fragments encompassing exons 5 to 9 (mutant 174, 270), exons 7 to 9 (mutants 238, 270 and 245, 270), and exons 8 and 9 (mutant 270, 306) were cloned into a plasmid, amplified in bacteria, and mutations determined by primer extension assay as described in Materials and Methods.

tumors. Remarkably, CC → TT mutations, which constitute 50% of all double substitutions in tumors (Table 5; ref. 10), were absent in patches. The data suggest that tandem double substitution mutations may be formed with a progressively higher frequency in later stages of the mouse tumor development.

These results show that all major mutation hotspots of the *p53* gene found in UVB-induced SCC are already present in epidermal cell patches long before the appearance of tumors and seem to persist in the genome with a similar incidence from early lesions to the late-stage tumors. Such a strong link indicates that p53-mutated skin patches constitute early precursors of SCCs.

Discussion

Patches of epidermal cells induced by chronic irradiation of hairless SKH-1 mice with UVB light and recognized by an antibody to the mutant form of p53 (PAb240) harbor identical p53 mutation hotspots as were observed in UVB-induced SCCs from the same model (10). Two hotspots in epidermal patches at codons 210 and 191 were not found in the previous major study of SCC. A difference in irradiation protocols could be a possible reason for this difference in mutational hotspots, with a significantly lower dose and frequency of irradiation used in our study (30 mJ/cm^2, twice a week for 20 weeks) than in ref. (10) (150 mJ/cm^2, five times a week for 18-25 weeks). Interestingly, in a separate study, 2 of 14 tumors induced by a solar simulator in hairless mice harbored a mutation at codon 210 (Arg → Cys). Although 92% of the simulator energy is in the UVA region and only 8% in the UVB region (12), the contribution of UVA light to the formation of this mutation is unlikely because the base substitution C → T is not a UVA-induced mutation but rather a UVB-induced mutation.

Another potential factor that could explain the absence of the two mutant hotspots in the Dumaz et al. study (10) is the use of different antibodies for the visualization of p53 protein: a monoclonal antibody PAb240 in our study of patches and a polyclonal antibody CM-5 in the study by Dumaz et al. (10). The PAb240 antibody recognizes a five-amino-acid epitope 210-RHSVV that is cryptic in normal murine p53 but exposed by a conformation change in mutant forms of p53 proteins, whereas CM-5 recognizes both the normal p53 conformation (29) and the mutant conformation represented by the PAb240 epitope (30). Therefore, CM-5 is likely to be more universal and should react with all mutant forms recognized by PAb240, including mutants at codons 191 and 210. It is interesting that the mutation at codon 210 changes arginine to cysteine in the first position of the PAb240 epitope, but such a change does not seem to prevent it from being recognized by the antibody in our study. It has been shown that the substitution of arginine for glutamic acid at position 210 abolishes immunoprecipitation of the mutant p53 by PAb240 antibody (31).

It is tempting to hypothesize that p53 proteins with mutations at codons 210 or 191 exhibit features that prevent a keratinocyte patch from developing into SCC. Interestingly, both tumors mutated at codon 210 by the solar simulator also harbored two other mutations with at least one being a major p53 hotspot (12) and therefore the mutation observed at codon 210 might not have contributed to the development of SCC. Functional studies of many human p53 mutants have shown wide variation in their transcription transactivation functions towards various target response elements making most mutants functionally unique (32, 33). Such a diversity of p53 transcriptional responses likely results in a variety of phenotypic outcomes. We assume that the incidence of mutations in tumors would mirror their incidence in patches increased or decreased by a factor reflecting their tumorigenicity. Based on our results, mutations at codons 191 and 210 would thus lie opposite from the mutations at codon 275 in a hypothetical spectrum of tumorigenicity, whereas other mutation hotspots (codons 270, 149, and 176) might be functionally similar, at least in their contribution to the development of SCC.

Tumor suppressor genes must have both of their alleles inactivated to abolish protective functions of their protein products (34). This can be achieved by alterations in both alleles (point mutations or deletions) or by an alteration in one allele and loss of the second allele (loss of heterozygosity, LOH; ref. 35). Timing of these events is a subject of discussion (36) and may depend on a particular type of the tumor suppressor and affected tissue. It seems likely that for p53 tumor suppressor it is the mutation that is induced first, because many p53 mutations exhibit dominant-negative function over the wild-type p53 and/or a "gain-of-function" mutation phenotype (37) providing the cell with a growth advantage even in the presence of a normal *p53* allele. Such a scenario seems to function in patches of epidermal cells expressing the mutant form of p53. Whether loss of the remaining normal *p53* allele constitutes an additional step towards a skin tumor and whether this happens primarily by an additional mutation in the remaining normal allele or by an allelic loss (LOH) is not clear. In this study, we found that 22.4% of mutant patches harbored a homozygous mutation. Although LOH in the *p53* gene locus *17p13.1* is frequent in actinic keratoses (40%, ref. 38 and 64%, ref. 39) as well as in SCC (80%, ref. 38 and 53%, ref. 39), LOH was not observed in mutant immunopositive patches of human keratinocytes (20, 21, 38) and thus it is possible that homozygous mutations detected in our study result from induction of the same mutation in both *p53* alleles rather than LOH. The majority of these mutations (16.4%) were formed at codon 270 (Arg → Cys). Interestingly, the human counterpart of this mutation at codon 273 (Arg → Cys) was found dominant negative over the wild-type protein in yeast functional assays (40, 41). Our data indicate that this dominance is likely incomplete in UVB-induced skin patches and that skin keratinocytes bearing a heterozygous mutation at codon 270 may acquire an additional advantage by selecting against the remaining wild-type *p53* allele.

Table 4. Comparison of *p53* gene mutations detected in epidermal patches of chronically UVB-irradiated hairless mice to the mutations found in UVB- and solar simulator–induced mouse SCCs

Codon	Exon	Sequence*	Amino acid	No. mutations			
				Patches	Tumors†	Tumors‡	Tumors§
60	4	gCc → gGc	Ala → Gly	1			
62	4	ctc Cga → ctc Tga	Arg → Term	1			
95	4	Cct → Tct	Pro → Ser	1			
101	4	tac Cag → tac Tag	Gln → Term	1			
110	4	Ttc → Atc	Phe → Ile	1			
110	4	ttC → ttA	Phe → Leu	1			
118	4	tCT → TtA	Ser → Leu	1			
127	5	Ctc → Ttc	Leu → Phe	2	1		
149	5	Cca → Tca	Pro → Ser	8	11		1
174	5	cCc → cTc	Pro → Leu	1	2		
174	5	Ccc → Tcc	Pro → Ser	1	1		
176	5	cac Cat → cac Tat	His → Tyr	2	5	1	
191	6	CTt → TCt	Leu → Ser	2			
191	6	cTt → cAt	Leu → His	2			
210	6	ttt Cgc → ttt Tgc	Arg → Cys	7		2	
235‖	7	atg Tgt → atg Agt	Cys → Ser	1			
238	7	tCc → tTc	Ser → Phe	1	3		3
238	7	TCc → CTc	Ser → Leu	1			
245	7	aac Cgc → aac Tgc	Arg → Cys	1	2		1
245	7	aac Cgc → aac Ggc	Arg → Gly	1			
245	7	aac Cgc → aac Agc	Arg → Ser	1			
261	8	Ctt → Ttt	Leu → Phe	1	1		
262	8	cTg → cCg	Leu → Pro	1		1	
270	8	gtt Cgt → gtt Tgt	Arg → Cys	42	50	11	6
274‖	8	tGc → tTc	Cys → Phe	1	1		
275	8	cCt → cTt	Pro → Leu	2	12	3	1
275	8	Cct → Tct	Pro → Ser	2	11		
306	9	Ccc → Tcc	Pro → Ser	1			
No. mutations				88	156¶	21¶	17¶
No. mutant samples				67	108	14	13
Percentage of mutant samples				64.4	68.0	87.5	52.0
Percentage of 270 mutation				47.7	32.1	52.4	35.3

NOTE: The codon numbering originally reported in refs. (10, 13) did not count the first three NH_2-terminal amino acids of the protein resulting in three-digit lower numbers compared with this study.

*Nontranscibed strand.

† Data converted to our format from ref. (10).

‡ Data taken from ref. (12).

§Data converted to our format from ref. (13).

‖Mutated bases located in non pyr-pyr sites.

¶Numbers are sums of all mutations from the original report.

It was of considerable interest that only 64% of p53-immunopositive patches of skin cells from our UVB-treated mice actually contained a mutation in the *p53* gene. Taking into account that we used antibody recognizing only the mutant form of p53 protein, analyzed the whole coding region of the *p53* gene, and applied direct sequencing methodology to avoid a possible mutation underestimate by a prescreening technique, this result is rather surprising. It is possible that not all the cells from our isolated patches were mutants and therefore some samples might have been contaminated with a level of normal p53 that could compromise the detection of mutations in our assay. We believe this possibility is unlikely. Analyzing mixed DNA fragments containing either a mutant (270 Arg → Cys) or wild-type sequence in various ratios, we determined that the detection limit of our direct sequencing methodology was 25% of a mutant sequence in the analyzed mixture (data not shown). Therefore, a heterozygous mutation in a patch consisting of >50% of mutated cells should have been detected. It is unlikely that our isolated patches contained >50% of normal cells so that all patches with a mutation should have been analyzed as mutants. A potential explanation for the lack of p53 mutation in some mutant p53–positive patches could come from the observation that the structural motif recognized by PAb240 antibody is quite common among many proteins including mouse telomerase reverse transcriptase (42) and therefore cross-reactivity of the antibody with other protein(s) expressed in expanding but p53 wild-type patches, could yield a false positive staining. A recent study analyzing the whole coding sequence of the *p53* gene from human skin patches found only

Table 5. Incidence of base substitutions in mutations of the *p53* gene in UVB-induced epidermal cell patches and SCCs in SKH-1 mice

	Patches (%)	Tumors* (%)
Single substitutions		
GC → AT	75 (89.3)	117 (83.6)
GC → TA	2	7
GC → CG	2	
AT → GC	1	8
AT → TA	4	4
Other		4
Total	84	140
Double substitutions		
CT → TC	2	
CT → TA	1	3
TC → CT	1	
CC → TT		8
Other		5
Total	4 (4.5)	16 (10.3)
Location of substitutions		
Dipyrimidine site	86 (97.7)	150 (96.2)
Nondipyrimidine site	2	6
Dipyrimidine site location		
Nontranscribed strand	86 (100)	140 (93.3)
Transcribed strand		10

*Data recalculated from Dumaz et al (10).

57% of samples harboring a p53 mutation (22), which is very similar to our results. The patches were visualized with another monoclonal antibody, DO-7, recognizing both mutant and normal form of human p53. Therefore, the cross-reactivity of monoclonal antibodies with non-p53 proteins may provide a clue to these puzzling results. Another explanation stems from the observation that cells exposed to certain conditions change the wild-type conformation of p53 to the mutant form. Growth stimulation of blood cells with a mitogen (43) or differentiation of embryonic stem cells with all-*trans* retinoic acid (44) results in immunoreactivity of wild-type p53 protein with PAb240 antibody. It is therefore conceivable that chronic UV light irradiation could induce heritable cellular changes stabilizing the mutant conformation of the p53 protein that would compromise the wild-type p53 function without mutations in the *p53* gene. Whether factors like hsp90 or other molecular chaperones that bind to mutant (45) and wild-type p53 protein (46, 47), and stabilize it against degradation, could play a role in regulation of p53 protein conformation remains to be seen.

In conclusion, we showed that all p53 mutation hotspots from mouse skin SCC are already present in UVB-induced p53-positive epidermal cellular patches long before the formation of tumors and also that the majority of mutant patches (77.6%) harbors at least one tumor p53 mutation hotspot. In addition, we identified two mutant hotspots in skin patches not detected in SCC, and these mutant cells may not have the ability to form tumors or they may be eliminated before tumor formation. Our observation that only 64% of patches that stain with an antibody that recognizes conformationally altered p53 protein actually harbor a p53 mutation is intriguing and suggests that the patches without a p53 mutation consist of conformationally altered p53 protein or that the antibody cross reacts with other proteins that possess the same antigenic epitope as mutant p53. Our data confirm a strong genetic link between the patches and SCC in the mouse and support the view that patches constitute an early step towards the formation of skin SCCs.

Acknowledgments

Received 12/21/2004; accepted 2/25/2005.

Grant support: NIH grants CA80759 and CA88961.

The costs of publication of this article were defrayed in part by the payment of page charges. This article must therefore be hereby marked *advertisement* in accordance with 18 U.S.C. Section 1734 solely to indicate this fact.

References

1. Armstrong BK, Kricker A. The epidemiology of UV induced skin cancer. J Photochem Photobiol B 2001; 63:8–18.
2. de Gruijl FR, Forbes PD. UV-induced skin cancer in a hairless mouse model. Bioessays 1995;17:651–60.
3. de Gruijl FR, Sterenborg HJ, Forbes PD, et al. Wavelength dependence of skin cancer induction by ultraviolet irradiation of albino hairless mice. Cancer Res 1993;53:53–60.
4. van Kranen HJ, de Gruijl FR. Mutations in cancer genes of UV-induced skin tumors of hairless mice. J Epidemiol 1999;9:S58–65.
5. Giglia-Mari G, Sarasin A. p53 gene mutations in human skin cancers. Hum Mutat 2003;21:217–28.
6. Ziegler A, Jonason AS, Leffell DJ, et al. Sunburn and p53 in the onset of skin cancer. Nature 1994;372: 773–6.
7. Greenblatt MS, Bennett WP, Hollstein M, Harris CC. Mutations in the p53 tumor suppressor gene: clues to cancer etiology and molecular pathogenesis. Cancer Res 1994;54:4855–78.
8. Olivier M, Eeles R, Hollstein M, Khan MA, Harris CC, Hainaut P. The IARC TP53 database: new online mutation analysis and recommendations to users. Hum Mutat 2002;19:607–14.
9. Brash DE, Ziegler A, Jonason AS, Simon JA, Kunala S, Leffell DJ. Sunlight and sunburn in human skin cancer: p53, apoptosis, and tumor promotion. J Investig Dermatol Symp Proc 1996;1:136–42.
10. Dumaz N, van Kranen HJ, de Vries A, et al. The role of UV-B light in skin carcinogenesis through the analysis of p53 mutations in squamous cell carcinomas of hairless mice. Carcinogenesis 1997;18: 897–904.
11. Kanjilal S, Pierceall WE, Cummings KK, Kripke ML, Ananthaswamy HN. High frequency of p53 mutations in ultraviolet radiation-induced murine skin tumors: evidence for strand bias and tumor heterogeneity. Cancer Res 1993;53:2961–4.
12. Ananthaswamy HN, Fourtanier A, Evans RL, et al. p53 Mutations in hairless SKH-hr1 mouse skin tumors induced by a solar simulator. Photochem Photobiol 1998;67:227–32.
13. Queille S, Seite S, Tison S, et al. p53 mutations in cutaneous lesions induced in the hairless mouse by a solar ultraviolet light simulator. Mol Carcinog 1998;22: 167–74.
14. Jiang W, Ananthaswamy HN, Muller HK, Kripke ML. p53 protects against skin cancer induction by UV-B radiation. Oncogene 1999;18:4247–53.
15. Jonason AS, Kunala S, Price GJ, et al. Frequent clones of p53-mutated keratinocytes in normal human skin. Proc Natl Acad Sci U S A 1996;93:14025–9.
16. Berg RJ, van Kranen HJ, Rebel HG, et al. Early p53 alterations in mouse skin carcinogenesis by UVB radiation: immunohistochemical detection of mutant p53 protein in clusters of preneoplastic epidermal cells. Proc Natl Acad Sci U S A 1996;93:274–8.
17. Rebel H, Mosnier LO, Berg RJ, et al. Early p53-positive foci as indicators of tumor risk in ultraviolet-exposed hairless mice: kinetics of induction, effects of DNA repair deficiency, and p53 heterozygosity. Cancer Res 2001;61:977–83.
18. Zhang W, Remenyik E, Zelterman D, Brash DE, Wikonkal NM. Escaping the stem cell compartment: sustained UVB exposure allows p53-mutant keratinocytes to colonize adjacent epidermal proliferating units without incurring additional mutations. Proc Natl Acad Sci U S A 2001;98:13948–53.
19. Backvall H, Wolf O, Hermelin H, Weitzberg E, Ponten F. The density of epidermal p53 clones is higher adjacent to squamous cell carcinoma in comparison with basal cell carcinoma. Br J Dermatol 2004;150: 259–66.
20. Ren ZP, Hedrum A, Ponten F, et al. Human epidermal cancer and accompanying precursors have identical p53 mutations different from p53 mutations in adjacent areas of clonally expanded non-neoplastic keratinocytes. Oncogene 1996;12:765–73.
21. Ren ZP, Ahmadian A, Ponten F, et al. Benign clonal keratinocyte patches with p53 mutations show no genetic link to synchronous squamous cell precancer or cancer in human skin. Am J Pathol 1997;150:1791–803.
22. Backvall H, Stromberg S, Gustafsson A, Asplund A, Sivertsson A, Lundeberg J, et al. Mutation spectra of

epidermal p53 clones adjacent to basal cell carcinoma and squamous cell carcinoma. Exp Dermatol 2004;13:643–50.
23. Corpet F. Multiple sequence alignment with hierarchical clustering. Nucleic Acids Res 1988;16:10881–90.
24. Kramata P, Zajc B, Sayer JM, Jerina DM, Wei CS. A single site-specific *trans*-opened 7,8,9,10-tetrahydrobenzo[a]pyrene 7,8-diol 9,10-epoxide N^2-deoxyguanosine adduct induces mutations at multiple sites in DNA. J Biol Chem 2003;278:14940–8.
25. Sheffield VC, Beck JS, Kwitek AE, Sandstrom DW, Stone EM. The sensitivity of single-strand conformation polymorphism analysis for the detection of single base substitutions. Genomics 1993;16:325–32.
26. Moyret C, Theillet C, Puig PL, Moles JP, Thomas G, Hamelin R. Relative efficiency of denaturing gradient gel electrophoresis and single strand conformation polymorphism in the detection of mutations in exons 5 to 8 of the p53 gene. Oncogene 1994;9:1739–43.
27. Zhao K, Chai X, Johnston K, Clements A, Marmorstein R. Crystal structure of the mouse p53 core DNA-binding domain at 2.7 A resolution. J Biol Chem 2001;276:12120–7.
28. Brash DE, Rudolph JA, Simon JA, et al. A role for sunlight in skin cancer: UV-induced p53 mutations in squamous cell carcinoma. Proc Natl Acad Sci U S A 1991;88:10124–8.
29. Midgley CA, Owens B, Briscoe CV, Thomas DB, Lane DP, Hall PA. Coupling between γ irradiation, p53 induction and the apoptotic response depends upon cell type *in vivo*. J Cell Sci 1995;108:1843–8.
30. Lane DP, Stephen CW, Midgley CA, et al. Epitope analysis of the murine p53 tumour suppressor protein. Oncogene 1996;12:2461–6.
31. Stephen CW, Lane DP. Mutant conformation of p53. Precise epitope mapping using a filamentous phage epitope library. J Mol Biol 1992;225:577–83.
32. Resnick MA, Inga A. Functional mutants of the sequence-specific transcription factor p53 and implications for master genes of diversity. Proc Natl Acad Sci U S A 2003;100:9934–9.
33. Kato S, Han SY, Liu W, et al. Understanding the function-structure and function-mutation relationships of p53 tumor suppressor protein by high-resolution missense mutation analysis. Proc Natl Acad Sci U S A 2003;100:8424–9.
34. Vogelstein B, Kinzler KW. The multistep nature of cancer. Trends Genet 1993;9:138–41.
35. Thiagalingam S, Laken S, Willson JK, et al. Mechanisms underlying losses of heterozygosity in human colorectal cancers. Proc Natl Acad Sci U S A 2001;98:2698–702.
36. Wilentz RE, Argani P, Hruban RH. Loss of heterozygosity or intragenic mutation, which comes first? Am J Pathol 2001;158:1561–3.
37. Cadwell C, Zambetti GP. The effects of wild-type p53 tumor suppressor activity and mutant p53 gain-of-function on cell growth. Gene 2001;277:15–30.
38. Ahmadian A, Ren ZP, Williams C, et al. Genetic instability in the 9q22.3 region is a late event in the development of squamous cell carcinoma. Oncogene 1998;17:1837–43.
39. Rehman I, Takata M, Wu YY, Rees JL. Genetic change in actinic keratoses. Oncogene 1996;12:2483–90.
40. Brachmann RK, Vidal M, Boeke JD. Dominant-negative p53 mutations selected in yeast hit cancer hot spots. Proc Natl Acad Sci U S A 1996;93:4091–5.
41. Monti P, Campomenosi P, Ciribilli Y, et al. Tumour p53 mutations exhibit promoter selective dominance over wild type p53. Oncogene 2002;21:1641–8.
42. Shats I, Milyavsky M, Erez N, Rotter V. The murine telomerase catalytic subunit shares the PAb-240 mutant specific epitope of the p53 protein. FEBS Lett 2003;546:321–4.
43. Zhang W, Hu G, Estey E, Hester J, Deisseroth A. Altered conformation of the p53 protein in myeloid leukemia cells and mitogen-stimulated normal blood cells. Oncogene 1992;7:1645–7.
44. Sabapathy K, Klemm M, Jaenisch R, Wagner EF. Regulation of ES cell differentiation by functional and conformational modulation of p53. EMBO J 1997;16:6217–29.
45. Blagosklonny MV, Toretsky J, Bohen S, Neckers L. Mutant conformation of p53 translated *in vitro* or *in vivo* requires functional HSP90. Proc Natl Acad Sci U S A 1996;93:8379–83.
46. Walerych D, Kudla G, Gutkowska M, et al. Hsp90 chaperones wild-type p53 tumor suppressor protein. J Biol Chem 2004;279:48836–45.
47. Muller L, Schaupp A, Walerych D, Wegele H, Buchner J. Hsp90 regulates the activity of wild-type p53 under physiological and elevated temperatures. J Biol Chem 2004;279:48846–54.

Patches of Mutant p53-Immunoreactive Epidermal Cells Induced by Chronic UVB Irradiation Harbor the Same p53 Mutations as Squamous Cell Carcinomas in the Skin of Hairless SKH-1 Mice

Pavel Kramata, Yao-Ping Lu, You-Rong Lou, et al.

Cancer Res 2005;65:3577-3585.